Terahertz Near-Field Measurements of Small Metal Structures

Aurèle J. L. Adam[a], J. R. Knab[a], M. Nagel[b], M. A. Seo[c], D. S. Kim[c] and P. C. M. Planken[a]

[a] Delft University of Technology, Delft, The Netherlands

[b] Institut für Halbleitertechnik, RWTH Aachen University, Aachen, Germany

[c] School of Physics and Astronomy, Seoul National University, Seoul, Korea

***Abstract*—We present results on THz near-field measurements of sub-wavelength single holes made in metal. Time and frequency dependence of the electric near-field of single sub-wavelength apertures are compared with the near-field predictions made by the well-known Bethe-Bouwkamp model.**

I. Introduction

How does light diffract from a small aperture? This question is extremely relevant considering the recent discovery of the extraordinary transmission of light by aperture arrays.[1] Understanding the differences between the near-field and the far-field spectra of such structures is important for spectroscopic measurement.[2] In general, understanding how light propagates around small objects is important due to, for example, the effects of local field enhancement on various non-linear optical processes.[3] Thus far, measuring the electric near-field or subwavelength structures (hole, sphere, rod) has proven to be very difficult. Until recently, no techniques existed that were capable of measuring all the components of the electromagnetic near–field with an adequate spatial resolution and signal dynamic range.

Here, we present results from electric near-field measurements of subwavelength apertures in the THz domain, using the technique of terahertz time-domain spectroscopy (THz-TDS). Using this technique, we measure the three components of the near-field, E_x, E_y, E_z, in the vicinity of the structures for wave vectors k, corresponding to $ka \ll 1$, $ka \approx 1$ and $ka > 1$, with a the typical dimension of the structure.

II. Description of the Set-up

The set-up is based on a typical THz -TDS system.[4] THz pulses are generated in a GaAs photoconductive switch that is modulated with a 50 kHz square-wave voltage. THz light is focused onto our sample, which is fabricated directly on the Electro Optical (EO) detection crystal (see Fig. 1). The crystal is mounted on a *xy* computer-controlled, piezo-electric *x-y* translation stage with a 1 µm step size. From below, a counter propagating, synchronized probe laser pulse is focused onto the surface of the EO crystal using a reflective objective.

The probe beam is optically delayed with an in-plane retro-reflector, mounted on a loudspeaker that oscillates at 50 Hz. Due to the electro-optic effect, the THz electric field elliptically polarizes the probe beam, which is reflected from the front surface of the crystal. Once reflected, it is sent to a standard differential detection setup. For each pixel, we collect a 25 ps long THz electric-field transients.

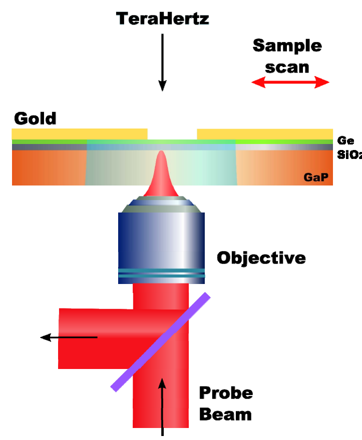

Fig. 1 Schematic of the setup used to measure the THz near-field of small metal objects. In this case the gold is directly deposited on the GaP EO crystal. The crystal can be raster scanned with respect to the probe/THz beam

The direct deposition of the structure on the EO crystal is the key for measuring the electric near-field around metallic structures with a high spatial resolution. The structure is made in a 200 nm-thick gold layer. The femtosecond probe laser pulse is focused on a ~5 µm diameter spot near the structure. The use of a <001> oriented GaP crystal enables us to measure only the *z*-component of the electric field while being blind to the *x* and *y* components. Using a <110> GaP crystal, we can measure the two components E_x and E_y of the electric field independently by rotating the crystal or the polarisation of the probe beam.[4] In principle, the three components of the electric field can be measured in the near field with subwavelength resolution using this technique.

III. Square Hole

The first measurement has been performed on a 200 µm square hole, made in a 200 nm thick gold film. Fig. 2 shows the near electric-field component, E_x, at two different frequencies: 200 GHz and 400 GHz. The incident field is polarized in the *x* direction. The spatial resolution is about 10 µm, much smaller than the typical THz wavelength. At 200 GHz, one can clearly see the shape of the square hole. The E_x component of the near electric field is stronger at the edges than at the center of the hole. In comparison, at 400 GHz, the E_x component of the near electric field is uniform in the hole and the square shape is less evident.

978-1-4244-2120-6/08/$25.00 ©IEEE.

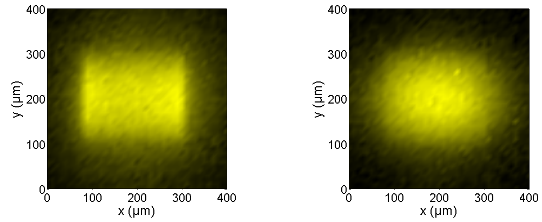

Fig. 2 Two dimensional maps of the THz electric near-field component, E_x, measured beneath a 200 µm square hole in a 200 nm thick gold film. On the left: f=200 GHz; on the right: f=400 GHz. Yellow indicates a high field amplitude, black a low field amplitude.

The choice of the frequency has been made so that in one case, the hole dimension is smaller than the wavelength and in the other case, the hole dimension is larger.

Fig. 3 shows the spectrum of the measured E_x component of the near electric field at the center of the hole. This spectrum is divided by the spectrum of the incident pulse. The maximum observed at 250 GHz is located close to the cut-off frequency of the lowest order mode of a rectangular waveguide, the TE_{10} mode, if we assume that hole is filled with a dielectric medium having the refractive-index of GaP (n=3.3).

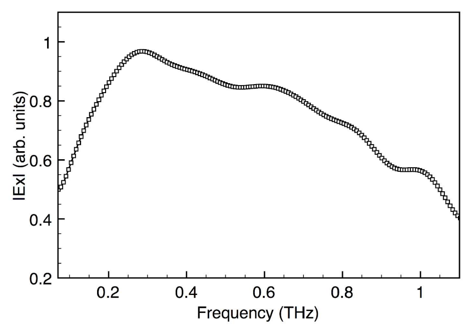

Fig. 3 Measured E_x component of the electric field at the center of the hole as a function of frequency. The spectrum is divided by the spectrum of the incident THz pulse.

In Fig. 4, we plot the *z*-component of the electric field at six different times, measured underneath the same square hole (200 µm). We clearly see the pulse emerging and spreading out from the hole. The THz pulse seems to propagate away from the edge as a spherical wave. Furthermore, the electric fields from opposite sides along the *x*-axis are pointing in opposite directions (different signs). Also note the small electric field on the top-left of each image. This is due to a small scratch in the gold layer through which some THz light can pass. One can see that the pairing of signs (or color) of the electric field for both holes is the same in the Fig. 4A (yellow on the left and black on the right), but is inverted in Fig. 4B. This provides additional information on how the hole reacts to the incident field with respect to its size. We will discuss this further in the following paragraph.

IV. Round Hole

The next measurement was performed on a 150 µm diameter round aperture, also made in a 200 nm thick gold film. In Fig. 5, we plot the *z*-component of the electric field, measured under the metal at four different times during the emergence of the THz pulse from the aperture.

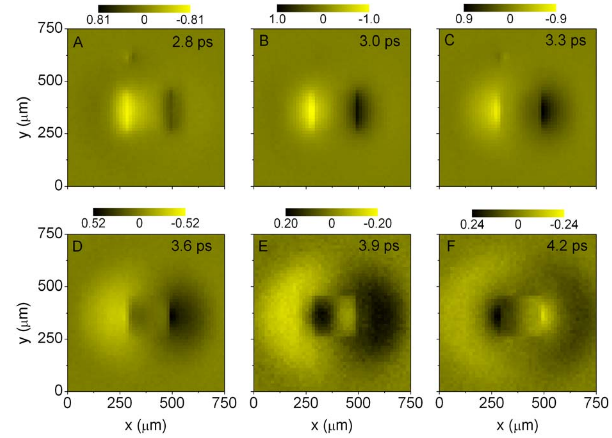

Fig. 4 (A-F) Two-dimensional maps of the THz electric near- field component E_x, measured beneath a 200 µm diameter hole in a 200 nm thick gold film, for six different times (indicated in the figures). Scale bars show the relative strengths of the measured fields. Yellow indicates negative electric fields, black indicates positive electric fields.

The incident field is polarized in the *x* direction. Fig. 5E shows two pulses of the electric field at two opposite edges of the holes. The pulses are opposite in sign. The images (A-D) in Fig. 5 show that directly underneath the hole, only a weak E_z component is observed. At the edges of the aperture, however, $|E_z|$ dramatically increases. This is manifest in Fig. 5F, where the electric field along the symmetry axis (x-axis) for different frequencies is plotted. FDTD calculations performed for this structure are in good agreement with the experiment.

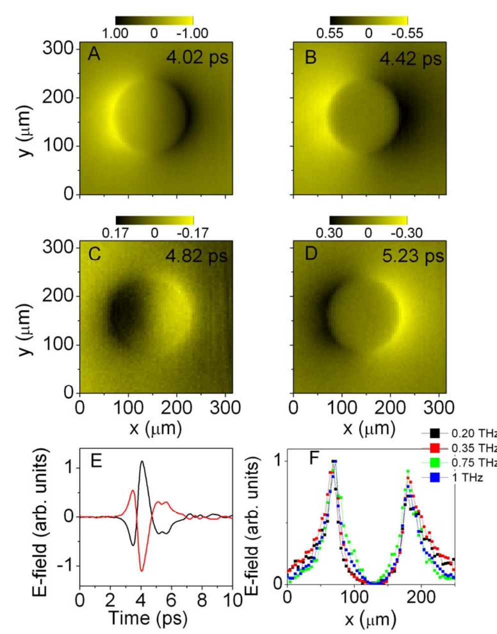

Fig. 5 (A-D) Two-dimensional maps of the THz electric near-field component, E_z, measured beneath a 150 µm diameter hole in a 200 nm thick gold film, for four different times (indicated in the figures). Scale bars show the relative strengths of the measured fields. Yellow indicates negative electric fields, black indicates positive electric fields. (E) Time-dependent electric field transients measured at the two opposite edges of the hole. (F) Electric field $|Ez|$, measured along the symmetry line, across a 100 µm diameter hole, for different frequencies.

This problem of diffraction of light by a subwavelength hole has been analytically calculated by Bethe[5] and later improved by Bouwkamp.[6] In Bouwkamp's model, the near-field *z*-component of the electric field of a hole at the shadow side of an infinitely thin, perfectly conducting metal, at $z = 0$ is written as:

$$E_z = E_0 \frac{4i}{3} ka \frac{a/\rho}{\sqrt{\rho^2/a^2 - 1}} \cos(\varphi)$$

with $\rho > a$,with a the radius of the hole, *r* the radial coordinate, φ the azimuthal angle, E_0 the electric field amplitude and *k* the wavevector of the incident radiation. One can see already that at the edge the electric field is infinite.

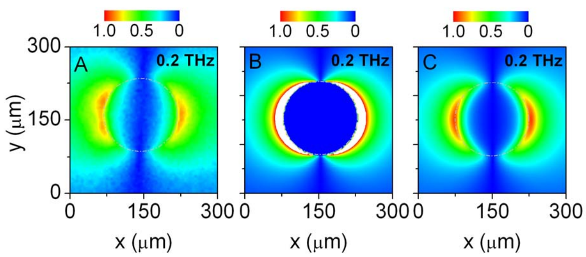

Fig. 6 (A) Measured spatial distribution of the z-component, $|E_z|$, of the electric field at 0.2 THz, behind a 150 µm hole in a 200 nm thick gold film, deposited on a GaP electro-optic crystal. (B) Spatial distribution of $|E_z|$, calculated using the Bouwkamp model. White indicates electric field values higher than the range of values indicated by the scale bar. (C) FDTD calculations showing the spatial distribution of $|E_z|$ at a distance of 10 µm below the metal.

Fig. 2 shows the spatial distribution of the *z*-component of the electric field, measured behind a 150 µm diameter hole at 0.2 THz (A), calculated with the Bouwkamp Model (B) and calculated using FDTD. One can see that the three graphs are similar and show the same dependence on the azimuthal angle, thus confirming one of the predictions by Bouwkamp.

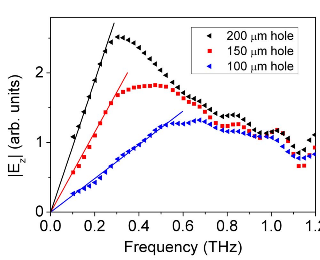

Fig. 7 Measured electric field at the edge of the hole as a function of frequency, for hole diameters of 100, 150, and 200 µm. The spectra are divided by the spectrum of the incident THz pulse.

In order to confirm the frequency-dependence of the near-field amplitude, we plot in Fig. 7 the frequency-dependent electric near-field amplitude, $|E_z|$, measured at the edge, for the three different hole diameters. The signals are divided by the spectrum of the incident THz pulse. For the 100, 150 and 200 µm diameter holes, maxima in the field measured at the edge are observed at approximately 0.6, 0.4 and 0.3 THz, respectively. These maxima are located close to the cut-off frequency of the lowest order mode of a circular waveguide, the TE_{11} assuming that the hole is filled with a dielectric medium having the refractive-index of GaP, n=3.3.

For frequencies below the cut-off, the amplitude depends linearly on frequency, which is consistent with the linear dependence on *k* in Bouwkamp's model. This means that the hole is differentiating the incident pulse for frequencies lower than the cut-off. A similar result has been observed by Mitrofanov et al., in an in-plane near-field measurement behind a sub-wavelength aperture, at a fixed position, using a dipole antenna[7].

V. Conclusion

We have presented measurements of the electric near field in the vicinity of metallic structures. We have measured on the three components of the near electric field for square and circular subwavelength holes. We compared our results with the Bouwkamp model for three different subwavelength-sized circular holes. This investigation will be useful not only for near field spectroscopy, but it will also increase our understanding of new ways to increase the field for non-linear optical applications.

Acknowledgment

This work was performed as part of the research program of the "Stichting voor Fundamenteel Onderzoek der Materie (FOM)", which is financially supported by the "Nederlandse Organisatie voor Wetenschappelijk Onderzoek (NWO) and as part of the EU TERANOVA Program (RCN-71835)". Research support from the Korean government (Korean Science and Engineering Foundation, Ministry of Science and Technology, Ministry of Commerce and Industry, and the Research Council of the City of Seoul) is also acknowledged.

References

[1] T.W. Ebbesen, H. J. Lezec, H. F. Ghaemi, T. Thio, P. A.Wolff, "Extraordinary optical transmission through sub-wavelength hole arrays," in *Nature*, vol. 391, 1998, pp. 667-669.

[2] B. Hecht et al., "Scanning near-field optical microscopy with aperture probes: Fundamentals and applications," in *J. Chem. Phys.* vol. 112, 2000, pp. 7761-7773.

[3] J. T. Bahns, F. Yan, D. Qiu, R. Wang, L. Chen, "Hole-Enhanced Raman Scattering,"in *Appl. Spectrosc.*, vol. 60, 2006, pp. 989-993.

[4] P. C. M. Planken, H.-K. Nienhuys, H. J. Bakker, and W. Th. Wenckebach, "Measurement and calculation of the orientation dependence of terahertz pulse detection in ZnTe," J.Opt. Soc. Am. B., vol. 18, 2001, pp 313–317.

[5] H. A. Bethe, "Theory of diffraction by small holes, " Phys. Rev., vol. 66, 1944, pp. 163-182.

[6] C. J. Bouwkamp, "On Bethe's theory of diffraction by small holes," *Philips Res. Rep.*, Vol. 5, 1950, pp. 321-332.

[7] O. Mitrofanov, L. N. Pfeiffer, and K. W. West, "Generation of low-frequency components due to phase-amplitude modulation of subcycle far-infrared pulses in near-field diffraction," Appl. Phys. Lett., vol. 81, 2002, pp. 1579-1581.